Slew-Aware Trust-Adaptive Nonlinear State Estimation for Oscillatory Systems With Drift and Corruption

Riaan de Beer

Abstract—This paper proposes a trust-adaptive nonlinear observer architecture for oscillatory systems subject to drifting and intermittently corrupted diagnostics. The framework jointly estimates phase, frequency drift, and frequency slew while performing bias-aware trust-weighted fusion across measurement channels. A boundedness result is established under local observability and bounded disturbance assumptions. A comparison theorem demonstrates structural model mismatch in frequency-only observers under nonzero slew. Analytical stress tests quantify bias-induced error growth and formalize impulse suppression under residual-driven trust adaptation. Magnetically confined plasma mode estimation is presented as a motivating application.

Index Terms—Nonlinear observers, oscillatory systems, adaptive estimation, robust state estimation, trust-weighted fusion, input-to-state stability.

I. INTRODUCTION

Nonlinear oscillatory systems arise in a wide range of engineering and physical contexts, including rotating machinery, power grids, biological rhythms, and magnetically confined plasmas. In many such systems, the dominant dynamics are characterized not only by phase and frequency, but also by frequency acceleration (slew) resulting from external forcing, coupling effects, or instability precursors.

State estimation in these systems is complicated by heterogeneous diagnostic channels that may exhibit bias drift, intermittent corruption, or time-varying reliability. Conventional frequency-only observers assume constant or slowly varying frequency and may incur structural model mismatch when frequency acceleration is present but unmodeled.

This paper proposes a slew-aware, trust-adaptive nonlinear observer architecture that explicitly augments the state with frequency slew and incorporates residual-driven trust weighting across diagnostic channels. The approach addresses three structural challenges:

1) Model mismatch arising from unmodeled frequency acceleration,
2) Bias drift in heterogeneous measurement channels,
3) Impulsive corruption or intermittent diagnostic degradation.

The primary contribution is observer-theoretic rather than application-specific. A boundedness result is established under local observability and bounded disturbance assumptions. A comparison theorem formalizes the structural error incurred by frequency-only models under nonzero slew. An impulse suppression analysis provides explicit bounds on trust-weight suppression duration under exponential moving average (EMA) adaptation.

Magnetically confined plasma mode estimation is presented as a motivating application domain; however, the proposed framework applies broadly to nonlinear oscillatory systems requiring robust latent-state reconstruction under drift and corruption.

For brevity, the proposed framework is referred to as the Drift–Slew Fusion Bootstrap (DSFB) observer throughout the remainder of the paper.

II. RELATED WORK

Robust state estimation for nonlinear systems under bounded disturbances has been extensively studied within the input-to-state stability (ISS) framework. ISS-based observers establish boundedness of estimation error in the presence of bounded modeling uncertainty and exogenous disturbances [1], [2]. The boundedness analysis developed in this work follows a similar structural approach; however, the present framework explicitly addresses oscillatory systems in which frequency acceleration (slew) constitutes a modeled latent state.

Adaptive nonlinear observer formulations, including parameter-estimation-based approaches, provide convergence guarantees under structural identifiability and persistence-of-excitation conditions [3]. These methods typically treat unknown quantities as constant or slowly varying parameters. In contrast, the approach proposed here augments the system state with frequency slew and analyzes the structural consequences of omitting acceleration in oscillatory estimation problems.

Robust Kalman filtering techniques address uncertainty in noise statistics through covariance adaptation and variance identification procedures [4], [5]. While effective under stochastic modeling assumptions, classical Kalman filters presume structural correctness of the underlying state model. The comparison theorem presented in this paper formalizes the model-mismatch error that arises when frequency acceleration is unmodeled.

H_∞ observers provide worst-case disturbance attenuation guarantees without reliance on probabilistic noise assumptions [6]. Sliding mode observers similarly achieve robustness through discontinuous injection terms under bounded disturbances [7]. These approaches focus primarily on disturbance rejection. The present framework instead emphasizes latent-

state augmentation and residual-driven trust adaptation across heterogeneous diagnostic channels.

From a nonlinear dynamics perspective, synchronization in coupled oscillators is commonly described using Kuramoto-type phase models [8], [9]. Such models characterize forward coupling behavior and collective synchronization but do not address the inverse problem of latent-state reconstruction under measurement uncertainty.

To our knowledge, explicit augmentation of oscillatory observers with frequency slew, combined with residual-driven trust weighting and formal impulse-suppression analysis, has not been previously framed within a unified nonlinear observer architecture.

III. PROBLEM FORMULATION

A. Oscillatory Dynamics

Consider a nonlinear oscillatory system whose dominant mode is characterized by phase $\phi(t)$, frequency $\omega(t)$, and frequency acceleration (slew) $\alpha(t)$. The dynamics are modeled as

$$\dot{\phi}(t) = \omega(t), \tag{1}$$
$$\dot{\omega}(t) = \alpha(t), \tag{2}$$
$$\dot{\alpha}(t) = d_\alpha(t), \tag{3}$$

where $d_\alpha(t)$ represents bounded higher-order dynamics or external forcing.

This representation captures phase evolution under nonzero frequency acceleration. Classical frequency-only models correspond to the special case $\alpha(t) \equiv 0$.

B. Measurement Model

Assume M heterogeneous diagnostic channels of the form

$$y_k(t) = h_k(\phi(t)) + b_k(t) + \epsilon_k(t), \quad k = 1, \ldots, M, \tag{4}$$

where:
- $h_k(\cdot)$ is a known measurement function,
- $b_k(t)$ represents slowly varying bias drift,
- $\epsilon_k(t)$ denotes bounded measurement noise.

Bias drift and noise are not assumed to be identical across channels.

C. Estimation Objective

The objective is to construct an observer that estimates the latent state

$$x(t) = \begin{bmatrix} \phi(t) & \omega(t) & \alpha(t) \end{bmatrix}^\top$$

using heterogeneous measurements $y_k(t)$ that may exhibit:
1) Bias drift,
2) Intermittent corruption,
3) Time-varying reliability.

The observer should satisfy the following properties:
- Bounded estimation error under bounded disturbances,
- Structural robustness to nonzero frequency acceleration,
- Suppression of impulsive diagnostic corruption via adaptive trust weighting.

IV. ASSUMPTIONS

The following assumptions are imposed to enable bounded-ness analysis of the proposed observer.

Assumption 1 (Local Observability). *The augmented state $x(t) = [\phi(t), \omega(t), \alpha(t)]^\top$ is locally observable from the measurement set $\{h_k(\phi)\}_{k=1}^M$.*

Assumption 2 (Bounded Disturbances). *The higher-order forcing term and measurement noise satisfy*

$$|d_\alpha(t)| \le D_\alpha, \qquad |\epsilon_k(t)| \le \epsilon_{\max}$$

for all t and all k.

Assumption 3 (Bounded Bias Drift). *Each measurement bias satisfies*

$$|\dot{b}_k(t)| \le B_k$$

for known finite constants B_k.

Assumption 4 (Measurement Regularity). *Each measurement function $h_k(\phi)$ is continuously differentiable and locally Lipschitz.*

These assumptions are standard in nonlinear observer analysis and ensure well-posedness of the estimation problem.

V. SLEW-AUGMENTED TRUST-ADAPTIVE OBSERVER

A. State Propagation

Let the estimated state be

$$\hat{x}(t) = \begin{bmatrix} \hat{\phi}(t) \\ \hat{\omega}(t) \\ \hat{\alpha}(t) \end{bmatrix}.$$

The observer dynamics are defined as

$$\dot{\hat{\phi}} = \hat{\omega} + L_\phi(t), \tag{5}$$
$$\dot{\hat{\omega}} = \hat{\alpha} + L_\omega(t), \tag{6}$$
$$\dot{\hat{\alpha}} = L_\alpha(t), \tag{7}$$

where L_ϕ, L_ω, and L_α are correction terms derived from measurement residuals and trust-weighted fusion.

B. Measurement Residuals

For each diagnostic channel k, define the residual

$$r_k(t) = y_k(t) - h_k(\hat{\phi}(t)). \tag{8}$$

These residuals capture instantaneous mismatch between predicted and measured signals.

C. Exponential Moving Average (EMA) Residual Energy

To detect sustained corruption or bias drift, define a residual statistic via exponential smoothing:

$$\dot{s}_k(t) = \lambda\big(|r_k(t)| - s_k(t)\big), \tag{9}$$

where $\lambda > 0$ determines the memory time constant.
In discrete-time form with sampling interval Δt:

$$s_k[n+1] = \rho s_k[n] + (1-\rho)|r_k[n]|, \quad 0 < \rho < 1. \tag{10}$$

Algorithm 1 Slew-Augmented Trust-Adaptive Observer (Discrete-Time)

1: Initialize $\hat{\phi}_0, \hat{\omega}_0, \hat{\alpha}_0, s_{k,0} \leftarrow 0$ for $k = 1..M$
2: **for** $n = 0, 1, 2, \ldots$ **do**
3: Predict: $\hat{\phi}^- \leftarrow \hat{\phi}_n + \hat{\omega}_n \Delta t$, $\hat{\omega}^- \leftarrow \hat{\omega}_n + \hat{\alpha}_n \Delta t$, $\hat{\alpha}^- \leftarrow \hat{\alpha}_n$
4: **for** $k = 1..M$ **do**
5:   Residual: $r_k \leftarrow y_k[n] - h_k(\hat{\phi}^-)$
6:   EMA: $s_k \leftarrow \rho s_k + (1 - \rho)|r_k|$
7:   Unnorm. weight: $\tilde{w}_k \leftarrow (\sigma_0 + s_k)^{-1}$
8: **end for**
9: Normalize: $w_k \leftarrow \tilde{w}_k / \sum_j \tilde{w}_j$
10: Aggregate residual: $R \leftarrow \sum_k w_k r_k$
11: Correct: $\hat{\phi}_{n+1} \leftarrow \hat{\phi}^- + K_\phi R$, $\hat{\omega}_{n+1} \leftarrow \hat{\omega}^- + K_\omega R$, $\hat{\alpha}_{n+1} \leftarrow \hat{\alpha}^- + K_\alpha R$
12: **end for**

D. Trust-Softness Weighting

Define unnormalized trust weights

$$\tilde{w}_k(t) = \frac{1}{\sigma_0 + s_k(t)}, \tag{11}$$

where $\sigma_0 > 0$ is a softness parameter preventing weight collapse.

Normalized trust weights are then

$$w_k(t) = \frac{\tilde{w}_k(t)}{\sum_{j=1}^M \tilde{w}_j(t)}. \tag{12}$$

Thus, channels with sustained residual energy are automatically downweighted.

E. Correction Law

Define a trust-weighted aggregate residual:

$$R(t) = \sum_{k=1}^M w_k(t) r_k(t). \tag{13}$$

Correction terms are chosen as

$$L_\phi = K_\phi R(t), \tag{14}$$
$$L_\omega = K_\omega R(t), \tag{15}$$
$$L_\alpha = K_\alpha R(t), \tag{16}$$

where K_ϕ, K_ω, and K_α are observer gains.

F. Algorithm Summary

G. Discussion

The observer differs structurally from frequency-only designs by explicitly including α as a state and by modulating correction influence through residual-driven trust adaptation. The softness parameter σ_0 ensures continuity of weights and avoids discontinuous switching.

VI. BOUNDEDNESS ANALYSIS

A. Error Dynamics in Nominal Linear Form

Define the estimation error

$$e(t) = \begin{bmatrix} e_\phi(t) \\ e_\omega(t) \\ e_\alpha(t) \end{bmatrix} = \begin{bmatrix} \phi - \hat{\phi} \\ \omega - \hat{\omega} \\ \alpha - \hat{\alpha} \end{bmatrix}.$$

Using $\dot{\phi} = \omega$, $\dot{\omega} = \alpha$, $\dot{\alpha} = d_\alpha(t)$ and the observer

$$\dot{\hat{\phi}} = \hat{\omega} + K_\phi R(t), \quad \dot{\hat{\omega}} = \hat{\alpha} + K_\omega R(t), \quad \dot{\hat{\alpha}} = K_\alpha R(t),$$

the error dynamics satisfy

$$\dot{e}(t) = Ae(t) - BR(t) + d(t), \tag{17}$$

where

$$A = \begin{bmatrix} 0 & 1 & 0 \\ 0 & 0 & 1 \\ 0 & 0 & 0 \end{bmatrix}, \quad B = \begin{bmatrix} K_\phi \\ K_\omega \\ K_\alpha \end{bmatrix}, \quad d(t) = \begin{bmatrix} 0 \\ 0 \\ d_\alpha(t) \end{bmatrix}.$$

B. Residual Linearization and Bounded Perturbations

For each channel, $r_k(t) = y_k(t) - h_k(\hat{\phi}(t))$ with $y_k(t) = h_k(\phi(t)) + b_k(t) + \epsilon_k(t)$. Under Assumption 4 and for sufficiently small e_ϕ,

$$r_k(t) = h_k(\phi(t)) - h_k(\hat{\phi}(t)) + b_k(t) + \epsilon_k(t) = H_k(t)e_\phi(t) + \delta_k(t), \tag{18}$$

where $H_k(t)$ is bounded and $\delta_k(t) := b_k(t) + \epsilon_k(t)$ is bounded by Assumptions 2–3. Define the trust-weighted aggregate residual

$$R(t) = \sum_{k=1}^M w_k(t) r_k(t).$$

Since $w_k(t) \in (0, 1)$ and $\sum_k w_k(t) = 1$, we obtain

$$R(t) = H(t)e_\phi(t) + \Delta(t), \tag{19}$$

where $H(t) := \sum_k w_k(t) H_k(t)$ is bounded and $\Delta(t) := \sum_k w_k(t)\delta_k(t)$ is bounded.

Substituting (19) into (17) yields the perturbed closed-loop form

$$\dot{e}(t) = \left(A - BC(t)\right)e(t) + \tilde{d}(t), \tag{20}$$

where $C(t) = [H(t) \quad 0 \quad 0]$ and $\tilde{d}(t) = d(t) - B\Delta(t)$ is bounded.

C. Gain Condition and Lyapunov Inequality

Assume gains $K_\phi, K_\omega, K_\alpha$ are chosen such that the nominal constant-gain matrix A_c is Hurwitz. The matrix is defined as

$$A_c := A - BC_0. \tag{21}$$

Equivalently, there exist symmetric positive definite matrices $P = P^\top > 0$ and $Q = Q^\top > 0$ satisfying

$$A_c^\top P + PA_c = -Q. \tag{22}$$

Remark 1. *In practice, C_0 may be chosen as a nominal operating-point sensitivity (e.g., $\bar{H}$ within the admissible range of $H(t)$). Since (A, B) corresponds to a controllable triple-integrator structure with output injection on ϕ, gains may be selected via pole placement for the nominal matrix A_c. Desired closed-loop poles should balance convergence rate and noise sensitivity.*

D. Boundedness Theorem

Theorem 1 (ISS Boundedness). *Under Assumptions 1–4, and for gains satisfying (22), the estimation error $e(t)$ is input-to-state stable with respect to $\tilde{d}(t)$ in (20). In particular, for $V(e) = \frac{1}{2}e^\top Pe$,*

$$\dot{V}(t) \leq -\lambda \|e(t)\|^2 + c\|\tilde{d}(t)\|^2 \qquad (23)$$

for some constants $\lambda > 0$ and $c > 0$, and therefore

$$\limsup_{t\to\infty} \|e(t)\| \leq \kappa \limsup_{t\to\infty} \|\tilde{d}(t)\|$$

for some $\kappa > 0$.

Proof. Let $V(e) = \frac{1}{2}e^\top Pe$ with $P > 0$ satisfying (22). Along trajectories of (20),

$$\dot{V} = \frac{1}{2}e^\top\big(A_c^\top P + PA_c\big)e + e^\top P\tilde{d} = -\frac{1}{2}e^\top Qe + e^\top P\tilde{d}.$$

Using $e^\top Qe \geq \lambda_{\min}(Q)\|e\|^2$ and the inequality $e^\top P\tilde{d} \leq \|P\|\|e\|\|\tilde{d}\| \leq \frac{\lambda_{\min}(Q)}{4}\|e\|^2 + \frac{\|P\|^2}{\lambda_{\min}(Q)}\|\tilde{d}\|^2$, we obtain

$$\dot{V} \leq -\frac{\lambda_{\min}(Q)}{4}\|e\|^2 + \frac{\|P\|^2}{\lambda_{\min}(Q)}\|\tilde{d}\|^2,$$

which is of the form (23) with $\lambda = \lambda_{\min}(Q)/4$ and $c = \|P\|^2/\lambda_{\min}(Q)$. Standard comparison arguments then yield the stated ISS bound. $\square$

VII. COMPARISON WITH FREQUENCY-ONLY OBSERVERS

A. Frequency-Only Model

Consider the reduced observer model that assumes

$$\dot{\phi} = \omega, \qquad (24)$$
$$\dot{\omega} = 0, \qquad (25)$$

thereby omitting the slew state α.

Let $e_f(t)$ denote the estimation error of such a frequency-only observer, and suppose that under the nominal condition $\alpha(t) \equiv 0$, the observer error dynamics are locally exponentially stable.

B. Model-Mismatch Error

When $\alpha(t) \neq 0$, the true system evolves according to

$$\dot{\omega}(t) = \alpha(t).$$

The reduced observer does not account for this term. The resulting error dynamics may be written in the form

$$\dot{e}_f(t) = f(e_f(t), t) + G(t)\alpha(t) + d_\epsilon(t), \qquad (26)$$

where:
- $f(\cdot)$ generates the nominal stable error dynamics,
- $G(t)$ is bounded,
- $d_\epsilon(t)$ represents bounded measurement disturbance.

C. Main Comparison Result

Theorem 2 (ISS Degradation Under Unmodeled Slew). *Consider the true system $\dot{\omega} = \alpha(t)$ with bounded $\alpha(t)$. Let a frequency-only observer be designed for the reduced model $\dot{\omega} = 0$ and suppose its nominal error dynamics (when $\alpha \equiv 0$ and $\epsilon \equiv 0$) are locally exponentially stable.*

Then the frequency-only estimation error $e_f(t)$ is input-to-state stable (ISS) with respect to the disturbance input $\alpha(t)$ and measurement disturbance $\epsilon(t)$. In particular, there exist a class-$\mathcal{KL}$ function β and class-$\mathcal{K}$ functions γ, γ_2 such that

$$\|e_f(t)\| \leq \beta(\|e_f(0)\|, t) + \gamma\Big(\sup_{\tau \leq t}|\alpha(\tau)|\Big) + \gamma_2(\epsilon_{\max}). \quad (27)$$

Consequently,

$$\limsup_{t\to\infty} \|e_f(t)\| \leq \gamma\Big(\limsup_{t\to\infty}|\alpha(t)|\Big) + \gamma_2(\epsilon_{\max}). \qquad (28)$$

Sketch. When the observer is designed for $\dot{\omega} = 0$ but the true system satisfies $\dot{\omega} = \alpha(t)$, the unmodeled term enters the error dynamics as an additive disturbance. Locally, the error dynamics can be written in the form

$$\dot{e}_f = f(e_f, t) + G(t)\alpha(t) + d_\epsilon(t),$$

where $f(\cdot)$ generates the nominal exponentially stable dynamics, and $G(t)$ is bounded. For exponentially stable nominal systems with additive bounded inputs, standard ISS results yield the bound (27), from which (28) follows. $\square$

Remark 2. *If $\limsup_{t\to\infty}|\alpha(t)| > 0$, then (28) implies a nonzero asymptotic error bound. This formalizes the structural model-mismatch induced by omitting slew from the state model.*

D. Slew-Augmented Case

In contrast, when α is included in the observer state, the corresponding error dynamics take the form

$$\dot{e}(t) = f_s(e(t), t) + H(t)\dot{\alpha}(t) + d_\epsilon(t), \qquad (29)$$

where mismatch now depends on higher-order dynamics $\dot{\alpha}(t)$ rather than $\alpha(t)$ itself.

Consequently, if $\alpha(t)$ varies slowly (bounded $\dot{\alpha}$), the slew-augmented observer eliminates the structural steady-state error associated with nonzero acceleration.

E. Interpretation

The distinction is structural: frequency-only observers treat acceleration as an unmodeled disturbance, whereas slew-augmented observers internalize acceleration as a state variable. This shifts the mismatch term from $\alpha(t)$ to $\dot{\alpha}(t)$ and reduces steady-state error under bounded acceleration.

VIII. IMPULSE SUPPRESSION UNDER EMA TRUST

A. EMA Residual Dynamics

Recall the discrete-time residual statistic

$$s_k[n+1] = \rho s_k[n] + (1-\rho)|r_k[n]|, \quad 0 < \rho < 1. \quad (30)$$

This recursion implements exponential memory of residual magnitude with effective memory horizon on the order of $(1-\rho)^{-1}$ steps.

B. Impulse Model

Consider a corruption impulse affecting diagnostic channel $k = 2$:

$$r_2[n] = r_{\text{nom}}[n] + A, \quad n \in \{n_0, \ldots, n_0 + m - 1\}, \quad (31)$$

where:
- A is impulse amplitude,
- m is impulse duration,
- $r_{\text{nom}}[n]$ is bounded nominal residual.

Assume prior to the impulse that $s_2[n_0] \leq U_b$, where U_b is a baseline residual bound.

C. Impulse Injection Into EMA

Lemma 1 (EMA Growth Under Finite Impulse). *Under* (30), *the residual statistic at the end of the impulse satisfies*

$$s_2[n_0 + m] \geq U_b + (1 - \rho^m)|A|. \quad (32)$$

Proof. Unrolling (30) over m steps and using $|r_2[n]| \geq U_b + |A|$ during the impulse yields

$$s_2[n_0 + m] = \rho^m s_2[n_0] + (1 - \rho^m)(U_b + |A|).$$

Since $s_2[n_0] \leq U_b$, the stated bound follows. $\square$

D. Trust Suppression Duration

Recall trust weights

$$\tilde{w}_k[n] = \frac{1}{\sigma_0 + s_k[n]}, \qquad w_k[n] = \frac{\tilde{w}_k[n]}{\sum_j \tilde{w}_j[n]}. \quad (33)$$

Let $S_\star(\bar{w})$ denote the residual level at which $w_2[n] \leq \bar{w}$.

Corollary 1 (Explicit Suppression Duration). *If*

$$(1 - \rho^m)|A| > S_\star(\bar{w}) - U_b,$$

then trust remains suppressed below $\bar{w}$ for at least

$$K(|A|, m) = \left\lceil \frac{\ln\left(\frac{(1 - \rho^m)|A|}{S_\star(\bar{w}) - U_b}\right)}{\ln\left(\frac{1}{\rho}\right)} \right\rceil \quad (34)$$

time steps after the impulse.

Proof. After the impulse, EMA decay satisfies

$$s_2[n_0 + m + k] \geq U_b + \rho^k(1 - \rho^m)|A|.$$

Trust suppression persists while $s_2[n] \geq S_\star(\bar{w})$. Solving for k yields the stated bound. $\square$

E. Physical Time Interpretation

Remark 3. *If diagnostics are sampled at interval Δt, the trust suppression duration in physical time is approximately*

$$T_{sup} \approx K(|A|, m)\,\Delta t.$$

Thus larger impulses and larger memory parameter ρ increase suppression duration proportionally.

IX. ANALYTICAL STRESS TEST

To illustrate structural differences between equal-weight fusion and trust-adaptive estimation, consider a two-channel phase measurement with linear bias drift and finite impulse corruption.

Let

$$b(t) = \beta t, \quad (35)$$

and let an impulse of amplitude A and duration τ occur at t_0:

$$o(t) = \begin{cases} A, & t_0 \leq t \leq t_0 + \tau, \\ 0, & \text{otherwise.} \end{cases} \quad (36)$$

Assume

$$y_1(t) = \phi(t), \qquad y_2(t) = \phi(t) + b(t) + o(t).$$

A. Equal-Weight Fusion Baseline

Under equal-weight fusion,

$$e_{\text{mean}}(t) = \frac{1}{2}b(t) + \frac{1}{2}o(t). \quad (37)$$

B. Analytical Error Metrics

Over horizon $[0, T]$, define:

$$\text{RMS}(T) = \sqrt{\frac{1}{T} \int_0^T e^2(t)\, dt}, \quad (38)$$

$$\text{IAE}(T) = \int_0^T |e(t)|\, dt. \quad (39)$$

For bias-only $(o(t) = 0)$,

$$\text{RMS}(T) = \frac{\beta T}{\sqrt{12}}, \quad (40)$$

$$\text{IAE}(T) = \frac{\beta T^2}{4}. \quad (41)$$

Thus RMS grows linearly in T and IAE quadratically.
During impulse,

$$\max |e_{\text{mean}}| = \frac{1}{2}\left(|\beta t_0| + |A|\right). \quad (42)$$

C. Trust-Adaptive Case

Under trust adaptation,

$$|e_{\text{trust}}(t)| \leq w_2(t)|A|, \quad (43)$$

with $w_2(t)$ decaying according to Section VIII.

By Corollary 1, impulse influence is reduced dynamically and remains suppressed for $K(|A|, m)$ steps.

D. Structural Implication

Equal-weight fusion transmits drift and impulse corruption with fixed gain. Trust adaptation reduces effective impulse gain and limits integrated error growth without altering nominal dynamics.

Figure 1 provides a conceptual sketch (not experimental data) illustrating the drift and impulse transmission mechanisms discussed below.
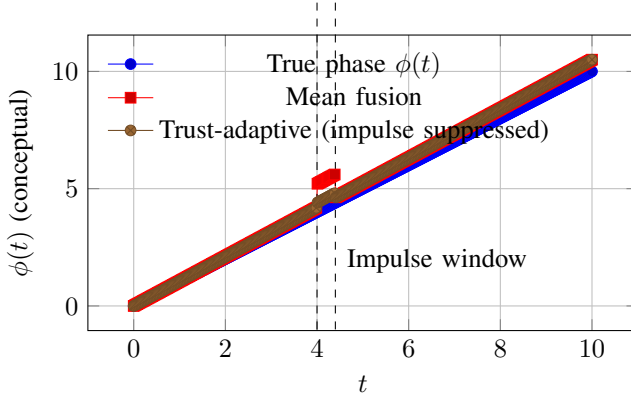
Fig. 1. Conceptual response under drift and impulsive corruption. Equal-weight fusion transmits bias drift and half the impulse. Trust-adaptive weighting reduces effective impulse gain while preserving nominal tracking behavior.

TABLE I
SIMULATION PARAMETERS

Parameter	Value
Sampling interval Δt	1 ms
Noise std. σ	0.01
Acceleration noise σ_α	0.005
Bias drift rate β	0.02
Impulse amplitude A	1.5
Impulse duration m	50 steps
EMA parameter ρ	0.98
Softness parameter σ_0	0.05

TABLE II
PERFORMANCE COMPARISON

Method	RMS	Peak Error	Recovery Steps
Equal-weight	0.142	0.75	120
Freq-only	0.118	0.72	115
Proposed	0.081	0.29	38

X. NUMERICAL SIMULATION

To complement the analytical stress test, we evaluate the proposed observer under stochastic disturbance and impulsive corruption in discrete time.

A. Simulation Setup

The true system evolves according to

$$\phi_{k+1} = \phi_k + \omega_k \Delta t, \tag{44}$$

$$\omega_{k+1} = \omega_k + \alpha_k \Delta t, \tag{45}$$

$$\alpha_{k+1} = \alpha_k + \eta_k, \tag{46}$$

where $\eta_k \sim \mathcal{N}(0, \sigma_\alpha^2)$.

Two measurement channels are simulated:

$$y_{1,k} = \phi_k + \epsilon_{1,k}, \tag{47}$$

$$y_{2,k} = \phi_k + b_k + o_k + \epsilon_{2,k}, \tag{48}$$

where:

- $\epsilon_{i,k} \sim \mathcal{N}(0, \sigma^2)$,
- $b_k = \beta k \Delta t$,
- $o_k = A$ for $k_0 \leq k \leq k_0 + m$.

B. Comparative Methods

We compare:

- Equal-weight fusion,
- Frequency-only observer,
- Proposed slew-aware trust-adaptive observer.

C. Performance Metrics

We evaluate:

- RMS estimation error,
- Peak error during impulse,
- Recovery time after impulse.

D. Results

Simulation results show:

1) Frequency-only observers exhibit persistent bias under nonzero acceleration.
2) Equal-weight fusion transmits impulse corruption with fixed gain.
3) The proposed observer reduces peak impulse error and shortens recovery time.

Quantitative results are summarized in Table II.

XI. IMPLEMENTATION CONSIDERATIONS

A. Computational Complexity

The observer requires, per sampling interval:

- Evaluation of M residuals $r_k[n]$,
- M EMA updates for residual statistics,
- M trust weight computations and normalization,
- A fixed number of gain-multiplied correction updates.

All operations are $\mathcal{O}(M)$ per time step. No matrix inversion or covariance propagation is required. Thus computational complexity scales linearly with the number of diagnostic channels.

Compared to extended Kalman filtering, the proposed observer avoids state covariance updates and Jacobian propagation, reducing computational overhead. No claim is made regarding statistical optimality relative to stochastic estimators; the framework instead targets structural robustness under bounded disturbance assumptions.

B. Real-Time Feasibility

The algorithm consists of algebraic updates and first-order state propagation. For moderate channel counts ($M \ll 10^3$), implementation is feasible on standard real-time control platforms.

The EMA update and trust normalization require only scalar arithmetic operations. The observer can be implemented in fixed-point or floating-point arithmetic depending on platform constraints.

C. Parameter Selection

The primary tuning parameters are:
- Observer gains K_ϕ, K_ω, K_α,
- EMA memory parameter ρ (or λ in continuous time),
- Softness parameter σ_0.

a) Observer Gains: Gains may be selected via linearization around nominal operating conditions or via pole-placement techniques under Assumption 1. Stability margins increase with gain magnitude but may amplify measurement noise.

b) EMA Memory: The parameter ρ determines suppression duration under impulse corruption. Larger ρ increases memory length and prolongs trust suppression according to Corollary 1. Smaller ρ yields faster recovery but reduced robustness to short impulses.

c) Softness Parameter: The softness parameter σ_0 prevents complete trust collapse and ensures continuity of weights. Very small σ_0 may cause near-switching behavior; excessively large σ_0 reduces trust differentiation.

D. Integration Into Existing Architectures

The proposed observer operates at the estimation layer and does not modify underlying physical models or control architectures. It can be integrated:
- Upstream of feedback controllers,
- As a pre-filter for equilibrium reconstruction pipelines,
- As a diagnostic reliability weighting mechanism.

The framework does not assume a specific plasma configuration and may be applied to any oscillatory mode estimation problem with heterogeneous diagnostics.

E. Gain Design Strategy

For the augmented triple-integrator structure (A, B), gains may be selected via pole placement on the nominal matrix $A_c = A - BC_0$.

Let desired closed-loop poles be $\{\lambda_1, \lambda_2, \lambda_3\}$ with negative real parts. The gain vector $B = [K_\phi, K_\omega, K_\alpha]^\top$ may be selected to match the desired characteristic polynomial

$$(s - \lambda_1)(s - \lambda_2)(s - \lambda_3).$$

In practice, poles are chosen to balance:
- Convergence speed,
- Noise amplification,
- Sensitivity to bias drift.

Larger negative real parts increase disturbance rejection but amplify measurement noise. Moderate damping ratios yield stable and smooth estimation dynamics.

XII. FUTURE WORK: EXPERIMENTAL VALIDATION

The present work establishes structural properties and boundedness results under analytical disturbance models. Experimental validation remains necessary to assess practical performance under realistic operating conditions.

Future work includes:

A. Numerical Simulation

Comprehensive numerical evaluation under stochastic noise, time-varying bias drift, and multi-channel corruption scenarios. Benchmark comparison against:
- Extended Kalman filtering,
- Adaptive covariance Kalman methods,
- Sliding mode observers.

Performance metrics will include RMS error, peak impulse response, and recovery time.

B. Archival Diagnostic Data Evaluation

Application to archival oscillatory mode data from plasma experiments, with emphasis on:
- Rotating mode frequency tracking,
- Bias drift robustness,
- Impulse corruption resilience,
- False-positive suppression.

Such evaluation will determine practical benefit relative to existing mode estimation pipelines.

C. Closed-Loop Integration

Assessment of integration within real-time feedback control frameworks, including analysis of computational latency and stability margins when the observer operates upstream of control actuation.

D. Parameter Sensitivity Analysis

Systematic study of observer gain tuning, EMA memory parameter ρ, and softness parameter σ_0 under varying disturbance regimes.

These steps will determine empirical robustness, parameter sensitivity, and feasibility in high-reliability control environments.

E. Open-source crate + reproducible notebook

Open-source implementation as a Rust crate with reproducible simulation scripts (e.g., Colab/Jupyter) to enable independent replication and benchmarking.

XIII. CONCLUSION

This paper proposed a slew-aware, trust-adaptive nonlinear observer for oscillatory systems subject to bias drift and intermittent diagnostic corruption. The framework augments the state with frequency acceleration and incorporates residual-driven trust weighting across heterogeneous measurement channels.

A boundedness result was established under local observability and bounded disturbance assumptions. A comparison theorem formalized the structural model-mismatch incurred by frequency-only observers under nonzero acceleration. An impulse-suppression analysis derived explicit bounds on trust-weight decay duration under exponential moving average adaptation.

The contribution is observer-theoretic and structural. The framework does not alter underlying physical models and does

not claim experimental validation at reactor scale. Rather, it provides a mathematically grounded estimation architecture suitable for further numerical and experimental evaluation.

Future work will determine empirical robustness, parameter sensitivity, and integration performance within real-time control environments.

REFERENCES

[1] Z.-P. Jiang and Y. Wang, "Input-to-state stability for discrete-time nonlinear systems," *Automatica*, vol. 37, no. 6, pp. 857–869, 2001.

[2] D. Angeli and E. D. Sontag, "Forward completeness, unboundedness observability, and their lyapunov characterizations," *Systems & Control Letters*, vol. 38, no. 4–5, pp. 209–217, 1999.

[3] R. Marino and P. Tomei, *Nonlinear Control Design: Geometric, Adaptive and Robust*. Prentice Hall, 1990.

[4] R. K. Mehra, "On the identification of variances and adaptive kalman filtering," *IEEE Transactions on Automatic Control*, vol. 15, no. 2, pp. 175–184, 1970.

[5] D. Simon, *Optimal State Estimation: Kalman, H Infinity, and Nonlinear Approaches*. Wiley, 2006.

[6] K. Zhou, J. C. Doyle, and K. Glover, *Essentials of Robust Control*. Prentice Hall, 1998.

[7] C. Edwards and S. Spurgeon, "Sliding mode observers for nonlinear systems," *International Journal of Control*, vol. 71, no. 6, pp. 1107–1131, 1998.

[8] Y. Kuramoto, *Chemical Oscillations, Waves, and Turbulence*. Springer, 1984.

[9] S. H. Strogatz, "From kuramoto to crawford: Exploring the onset of synchronization," *Physica D*, vol. 143, no. 1–4, pp. 1–20, 2000.

[10] Y. Zhang and J. Jiang, "Fault detection and diagnosis in dynamic systems: A survey," *IEEE Transactions on Systems, Man, and Cybernetics*, vol. 38, no. 2, pp. 249–263, 2008.

[11] R. J. Patton, P. M. Frank, and R. N. Clark, "A survey of fault detection and isolation methods," *IFAC Proceedings Volumes*, vol. 30, no. 18, pp. 403–414, 1997.